Spontaneous flexoelectric/flexomagnetic effect in nanoferroics

Eugene A. Eliseev,[1,*,†] Anna N. Morozovska,[1,*,‡] Maya D. Glinchuk,[1] and R. Blinc[2]
[1]*Institute for Problems of Materials Science, NAS of Ukraine, Krjijanovskogo 3, 03142 Kiev, Ukraine*
[2]*Jožef Stefan Institute, P.O. Box 3000, 1001 Ljubljana, Slovenia*
(Received 9 November 2008; revised manuscript received 25 February 2009; published 27 April 2009)

Within the Landau-Ginsburg-Devonshire phenomenological approach we study the ferroic nanosystem properties changes caused by the flexoeffect (flexoelectric and flexomagnetic) existing spontaneously due to the inhomogeneity of order parameters. An exact solution for the spatially inhomogeneous mechanical displacement vector allowing for flexocoupling contribution was found for nanowires and thin pills. Strong influence of the flexoeffect on nanorods and thin pills leads to the displacements of the atoms resulting into the unit-cell symmetry changes, which lead to the phase-transition temperature shift, as well as the nanoparticle shape distortions; in particular, flat cross sections transform into saucerlike ones. The phenomena can be considered as true manifestation of the spontaneous flexoeffect existence. It was shown that flexoeffect leads to (a) the appearance of linear and nonlinear contributions and renormalization of coefficients before the order-parameter gradient, (b) essentially influences the transition temperature, piezoelectric response, and the spatial distribution of the order parameter, and (c) results in renormalization of extrapolation length in the boundary conditions. These effects cannot be neglected for ferroelectrics, the renormalization being important for nanoparticles of arbitrary shape, while the linear and nonlinear terms are essential for the thin pills only. They are absent for nanowires with the order parameter directed along the wire axis. We demonstrated that the flexoelectric coupling decreases the polarization gradient self-consistently and so makes polarization more homogeneous. It was shown that revealed effect of the correlation radius renormalization by the flexoelectric effect leads to the renormalization of the intrinsic width of ferroelectric domain walls.

DOI: 10.1103/PhysRevB.79.165433 PACS number(s): 77.80.−e, 77.84.Dy, 68.03.Cd, 68.35.Gy

I. INTRODUCTION

The most general definition of the direct flexoeffect is the appearance of the polarization or magnetization in response to *inhomogeneous* mechanical impact (elastic stress or strain *gradient*). The converse flexoeffect corresponds to the appearance of mechanical stress or strain in response to the gradient of order parameter. Let us underline that flexocoupling affects both the system response to the external impact and the intrinsic gradient of order parameters. Typical example is flexoelectric effect[1–3] originated from the coupling of polarization gradient with elastic strain and polarization with elastic strain gradient. It is worth to underline that the flexomagnetic effect should exist in the materials with symmetry without inversion of time (e.g., in some antiferromagnetics[4]) so that the symmetry consideration for flexomagnetic effect will be similar to the well-studied flexoelectric phenomena.

The flexoelectric effect was predicted by Mashkevich and Tolpygo,[5] later on theoretical study of the flexoelectric effect in bulk crystals was performed by Tagantsev,[2,3] experimental measurements of flexoelectric tensor components were carried out by Ma and Cross[6–8] and Zubko *et al.*[9] Renovation of the theoretical description for the flexoelectric response of different nanostructures starts from the papers of Catalan and co-workers,[10,11] while recent achievements are presented in the papers of Majdoub *et al.*[12] and Kalinin and Meunier.[13] However, in these papers the flexoelectric effect was considered as a coupling between *intrinsic* polar properties (e.g., polarization) and the *extrinsic* factors like the misfit strain relaxation[10,11] or the system bending by external forces,[12,13] while the coupling between intrinsic parameters (i.e., spontaneous polarization gradient and strain) was not considered. The crucial role of the surface in all physical properties of nanosystems including the strong order-parameter gradients in ferroic nanostructures[14] inevitably leads to the noticeable *spontaneous flexocoupling*, almost negligible for bulk materials, since the order parameters are usually homogeneous in this case.

It is worth to underline that phenomenological approach which was broadly used in the world scientific literature for description of nanosystems[15,16] as well as in the majority of aforementioned theoretical papers needs the estimations of spatial scales where phenomenological approach is valid. For ferroelectrics the correlation radii determine the minimum possible scale of order parameter changes, so the phenomenological approach can be valid if the correlation radii would be higher than lattice constant. In more general case the critical sizes of the long-range order existence in ferroics derived on the basis of microscopic[17] and phenomenological calculations[18] are in reasonable agreement both with each other and with experimental observation of ferromagnetic critical size of 7–30 nm (Ref. 19) and the ferroelectric critical size of 1–10 nm.[20–22] So, keeping in mind that phenomenological approach is suitable for long-range order description, the critical sizes lay in the region from several lattice constants to several nanometers, the region of phenomenological approach validity is broad enough. For instance, Majdoub *et al.*[12,23] considered either the response of cantilever-shaped beam to external stress gradient or the dielectric properties of thin film taking into account the polarization gradient allowing for flexoelectric effect. They apply phenomenological macroscopic models to nanosized systems and compare obtained results with microscopic modeling (*ab initio* and molecular-dynamics simulations). Majdoub

et al.[12,23] found that results of the microscopic modeling are qualitatively (and in some cases quantitatively) reproduced by the phenomenological model taking into account the flexoelectricity and polarization gradient.

In this paper we study the ferroic nanostructure property changes caused by flexoeffect existing due to the inhomogeneous spatial distribution of the order parameter (see Secs. II and III). Using concrete example of nanoferroelectrics (mechanically free pills, rods, and wires), we demonstrate that the flexoelectric coupling influence the majority of properties and in particular decreases the polarization gradient self-consistently and so renormalizes the correlation radius and stabilizes the ordered phase (see Sec. IV).

II. BASIC EQUATIONS FOR FLEXOEFFECT CONTRIBUTION IN FERROIC NANOPARTICLES

For the description of flexocoupling in ferroic nanoparticles we will use the Landau-Ginsburg-Devonshire (LGD) phenomenological approach[24,25] with respect to the surface energy, gradient energy, depolarization or demagnetization fields, mechanical stress, and flexoeffect. Since in nanostructures the flexoeffects cause the *internal driving forces* via the order-parameter gradients, which perform the virtual work, we need to minimize the Helmholtz free energy F.[26–30] For ferroics with the second-order phase transition corresponding LGD expansion of bulk (F_V) and surface (F_S) parts of Helmholtz free energy F on the order parameter $\boldsymbol{\eta}$ and strain tensor components u_{ij} have the form

$$F_V\int_V d^3r\left[\frac{a_{ij}(T)}{2}\eta_i\eta_j+\frac{a_{ijkl}}{4}\eta_i\eta_j\eta_k\eta_l-\eta_i\left(E_{0i}+\frac{E_i^d}{2}\right)\right.$$
$$+\frac{g_{ijkl}}{2}\left(\frac{\partial\eta_i}{\partial x_j}\frac{\partial\eta_k}{\partial x_l}\right)-\frac{f_{ijkl}}{2}\left(\eta_k\frac{\partial u_{ij}}{\partial x_l}-u_{ij}\frac{\partial\eta_k}{\partial x_l}\right)-q_{ijkl}u_{ij}\eta_k\eta_l$$
$$\left.+\frac{c_{ijkl}}{2}u_{ij}u_{kl}+\frac{v_{ijklmn}}{2}\left(\frac{\partial u_{ij}}{\partial x_m}\frac{\partial u_{kl}}{\partial x_n}\right)\right],$$

$$F_S=\int_S d^2r\left(\frac{a_{ij}^S}{2}\eta_i\eta_j+\frac{a_{ijkl}^S}{4}\eta_i\eta_j\eta_k\eta_l+\mu_{\alpha\beta}^S u_{\alpha\beta}+d_{ijk}^S u_{ij}\eta_k\right.$$
$$\left.+\frac{w_{ijkl}^S}{2}u_{ij}u_{kl}+\cdots\right). \quad (1)$$

Coefficients $a_{ij}(T)$ explicitly depend on temperature T. Coefficients a_{ij}^S, a_{ijkl}, and a_{ijkl}^S are supposed to be temperature independent; constants g_{ijkl} and v_{ijklmn} determine the magnitude of the gradient energy. Tensors g_{ijkl}, a_{ijkl}, and a_{ijkl}^S are positively defined. Tensor w_{jklm}^S is the surface excess elastic moduli, $\mu_{\alpha\beta}^S$ is the surface stress tensor,[31,32] and d_{ijk}^S is the surface piezoelectric tensor.[2,33] q_{ijkl} is the bulk striction coefficients and c_{ijkl} are components of elastic stiffness tensor.[34]

Tensor f_{ijkl} is the flexocoupling coefficient tensor.[9,10] In fact, only the Lifshitz invariant $\frac{f_{ijkl}}{2}\left(\eta_k\frac{\partial u_{ij}}{\partial x_l}-u_{ij}\frac{\partial\eta_k}{\partial x_l}\right)$ is relevant for the bulk contribution. Rigorously speaking, the gradient terms like $v_{ijklmn}(\partial u_{ij}/\partial x_k)(\partial u_{lm}/\partial x_n)$, which was ignored in Refs. 10 and 11 for the ferroelectrics, are responsible for the stable smooth distribution of the order parameter at nonzero strain gradients since the presence of Lifshitz invariant essentially changes the stability conditions.[35] Namely, in the scalar case the inequality $f^2<gc$ should be valid for the stability of the order-parameter smooth distribution. We obtained that in the considered tensorial case the terms $v_{ijklmn}(\partial u_{ij}/\partial x_k)(\partial u_{lm}/\partial x_n)$ can be neglected under the condition $f_{klmn}^2<g_{ijkl}c_{ijmn}$.

$\mathbf{E}_0$ in Eq. (1) is external field coupled with the order parameter $\boldsymbol{\eta}$. $\mathbf{E}^d$ is depolarization or demagnetization field that appears due to the nonzero divergence $[\mathrm{div}(\boldsymbol{\eta})\neq 0]$ of order parameter $\boldsymbol{\eta}$ in confined systems.[36,37]

The equations of state $\delta F_V/\delta\eta_i=0$ and $\delta F_V/\delta u_{ij}=\sigma_{ij}$ (where σ_{jk} is the stress tensor and δ is the symbol of variation derivative) obtained by variation in the bulk free energy [Eq. (1)] should be solved along with the equations of mechanical equilibrium $\partial\sigma_{ij}(\mathbf{x})/\partial x_i=0$ and compatibility equations equivalent to the mechanical displacement vector u_i continuity.[38] Variation in the surface and bulk free energy [Eq. (1)] on η_i yields to Euler-Lagrange equations with the boundary conditions

$$\left(g_{kjim}n_k\frac{\partial\eta_m}{\partial x_j}+a_{ij}^S\eta_j+\frac{f_{jkim}}{2}u_{jk}n_m\right)\Bigg|_S=0. \quad (2)$$

Here n_k are components of the external normal to the ferroic surface. The most evident consequence of the flexocoupling is the inhomogeneous boundary conditions.

In order to demonstrate spontaneous flexoeffect contribution to the nanoferroic properties, hereinafter we neglect the surface excess elastic modules, surface stress tensor, and surface piezoelectric effect contributions into the surface energy [Eq. (1)]. We consider *mechanically free* nanoparticles without misfit dislocations, which should lead to the "external" flexoeffect only. The contribution of misfit dislocations into the flexoelectric effect in thin films was considered in detail by Catalan *et al.*[10,11]

Allowing for essential contribution of elastic strains u_{ij} into the free energy [Eq. (1)], let us first proceed with their calculations. Then obtained elastic solution should be substituted into the Euler-Lagrange equations for the order-parameter components η_j.

III. SPONTANEOUS FLEXOEFFECT INFLUENCE ON ELASTIC FIELDS IN NANOFERROICS

Hereinafter let us consider a ferroic nanorod with radius R, height h, and the axially symmetric one-component order parameter $\eta_3(z,\rho)$ directed along the rod axis z (hereinafter $\rho=\sqrt{x_1^2+x_2^2}$ and $z=x_3$ are cylindrical coordinates). The external field $\mathbf{E}=(0,0,E_0)$ is also directed along the z axis. Equations of mechanical equilibrium $\partial\sigma_{ij}(\mathbf{x})/\partial x_i=0$, rewritten for nonzero displacement vector components $u_z(z,\rho)$ and $u_\rho(z,\rho)$, allowing for equation of state $\delta F_V/\delta u_{ij}=c_{ijkl}u_{kl}-q_{ij33}\eta_3^2+f_{ij3l}\partial\eta_3/\partial x_l=\sigma_{ij}$, acquire the form (see Appendix A in Ref. 39)

$$c_{11}\frac{\partial^2 u_z}{\partial z^2}+c_{44}\left(\frac{1}{\rho}\frac{\partial u_z}{\partial \rho}+\frac{\partial^2 u_z}{\partial \rho^2}\right)+(c_{12}+c_{44})\left(\frac{\partial^2 u_\rho}{\partial \rho\,\partial z}+\frac{1}{\rho}\frac{\partial u_\rho}{\partial z}\right)$$
$$=2q_{11}\eta_3\frac{\partial \eta_3}{\partial z}-f_1(\eta_3), \tag{3}$$

$$c_{11}\frac{\partial^2 u_\rho}{\partial \rho^2}+\frac{c_{11}}{\rho}\left(\frac{\partial u_\rho}{\partial \rho}-\frac{u_\rho}{\rho}\right)+c_{44}\frac{\partial^2 u_\rho}{\partial z^2}+(c_{12}+c_{44})\frac{\partial^2 u_z}{\partial \rho\,\partial z}$$
$$=2q_{12}\eta_3\frac{\partial \eta_3}{\partial \rho}-f_2(\eta_3). \tag{4}$$

Here the functions $f_1(\eta_3)=f_{11}\frac{\partial^2\eta_3}{\partial z^2}+f_{44}(\frac{\partial^2\eta_3}{\partial\rho^2}+\frac{1}{\rho}\frac{\partial\eta_3}{\partial\rho})$ and $f_2(\eta_3)=(f_{12}+f_{44})\frac{\partial^2\eta_3}{\partial\rho\partial z}$ originated from flexoelectric effect. Voigt notations are used hereinafter. The nanorods are regarded mechanically free, thus the corresponding boundary conditions are $\sigma_{z\rho}|_{z=\pm h/2}=\sigma_{zz}|_{z=\pm h/2}=0$, $\sigma_{z\rho}|_{\rho=R}=0$, and $\sigma_{\rho\rho}|_{\rho=R}=0$.

The equation of state $\delta F_V/\delta\eta_3=0$ in Voigt notation has the form

$$\left\{\left[a_1-2\left(q_{11}\frac{\partial u_z}{\partial z}+q_{12}\left(\frac{\partial u_\rho}{\partial\rho}+\frac{u_\rho}{\rho}\right)\right)\right]\eta_3+a_{11}\eta_3^3-g_{11}\frac{\partial^2\eta_3}{\partial z^2}\right.$$
$$\left.-g_{12}\left(\frac{\partial^2\eta_3}{\partial\rho^2}+\frac{1}{\rho}\frac{\partial\eta_3}{\partial\rho}\right)\right\}$$
$$=E_0+E_3^d+f_3(u). \tag{5}$$

Here the term $f_3(u)=f_{11}\frac{\partial^2 u_z}{\partial z^2}+f_{44}(\frac{1}{\rho}\frac{\partial u_z}{\partial\rho}+\frac{\partial^2 u_z}{\partial\rho^2})+(f_{12}+f_{44})(\frac{\partial^2 u_\rho}{\partial\rho\partial z}+\frac{1}{\rho}\frac{\partial u_\rho}{\partial z})$ originates from the flexoeffect. Equation (5) should be supplemented by the boundary conditions (2)

$$\left\{\pm g_{11}\frac{\partial\eta_3}{\partial z}+a_1^S\eta_3\pm\left[\frac{f_{12}}{2}\left(\frac{u_\rho}{\rho}+\frac{\partial u_\rho}{\partial\rho}\right)+\frac{f_{11}}{2}\frac{\partial u_z}{\partial z}\right]\right\}_{z=\pm h/2}=0,$$

$$\left[g_{12}\frac{\partial\eta_3}{\partial\rho}+a_1^S\eta_3+\frac{f_{44}}{2}\left(\frac{\partial u_z}{\partial\rho}+\frac{\partial u_\rho}{\partial z}\right)\right]\Bigg|_{\rho=R}=0 \tag{6}$$

(the sign "–" for $z=-h/2$ and the sign "+" for $z=h/2$).

Note that the limiting case $h/R\to 0$ corresponds to the films and thin pills, while the case $R/h\to 0$ corresponds to the wire. Our further analysis will be performed in the two cases of thin pills and wires; films will be considered elsewhere.

The *analytical* solution for mechanical displacements in nanowires (i.e., at $R\ll h$, $\partial\eta_3/\partial z\approx 0$, and $\partial\eta_3/\partial\rho\neq 0$) was derived in Appendix B in Ref. 39 as

$$u_\rho=\rho\left[\frac{1}{\rho^2}\int_0^\rho\frac{q_{12}}{c_{11}}\eta_3^2(\tilde\rho)\tilde\rho d\tilde\rho\right.$$
$$\left.+\frac{(c_{11}^2-c_{11}c_{12}+2c_{12}^2)q_{12}-2c_{11}c_{12}q_{11}}{2c_{11}(c_{11}-c_{12})(c_{11}+2c_{12})}\overline{\eta_3^2}\right], \tag{7a}$$

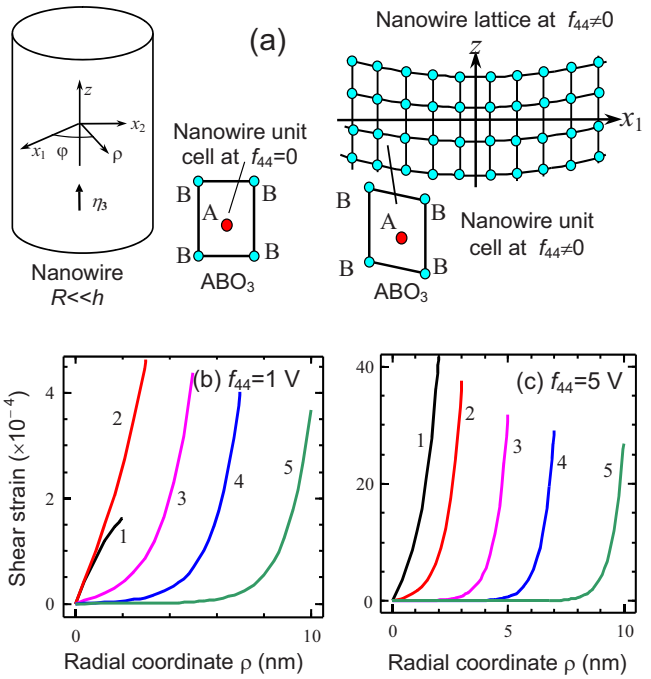

FIG. 1. (Color online) (a) Schematics of the perovskite ABO_3 lattice radial deformation from squire cross section to rectangular and incline parallelogram ones caused by spontaneous flexoeffect in nanowires. [(b) and (c)] Spontaneous shear strain $u_{\rho z}$ radial distribution inside the nanorod for flexoelectric coefficient (b) $f_{44}=1$ V and (c) 5 V. Nanorod radius values are $R=2$, 3, 5, 7, and 10 nm (curves 1–5). $PbTiO_3$ material parameters $T_c=479$ °C, $\alpha_T=3.8\times 10^5$ J m/C^2 K, $c_{44}=1.1\times 10^{11}$ J/m^3, $g_{12}=10^{-9}$ J m^3/C^2, and $\lambda_0=5$ nm and $a=0.4$ nm in Eq. (13b).

$$u_z=z\left[\frac{q_{11}(c_{11}+c_{12})-2q_{12}c_{12}}{(c_{11}-c_{12})(c_{11}+2c_{12})}\overline{\eta_3^2}\right]-\frac{f_{44}}{c_{44}}\eta_3, \tag{7b}$$

where $\overline{\eta_3^2}=\frac{2}{R^2}\int_0^R\eta_3^2(\tilde\rho)\tilde\rho d\tilde\rho$. Note that in-plane elastic strain $u_{\rho\rho}+u_{\psi\psi}=\frac{q_{12}}{c_{11}}(\eta_3^2-\overline{\eta_3^2})+\frac{2(c_{11}q_{12}-c_{12}q_{11})}{(c_{11}-c_{12})(c_{11}+2c_{12})}\overline{\eta_3^2}$ calculated from Eq. (7) is different from the homogeneous spontaneous strain components in bulk material, which are simply proportional to $\eta_3^2\equiv\overline{\eta_3^2}$.[36] Actually, the intrinsic term proportional to the difference $(\eta_3^2-\overline{\eta_3^2})$ absent in the bulk solution was omitted in the solution for films used in Refs. 10 and 11.

The substitution of the shear strain $u_{\rho z}=-\frac{f_{44}}{2c_{44}}\frac{\partial\eta_3}{\partial\rho}$ calculated from Eq. (7) into Eq. (5) leads to the gradient coefficient g_{12} renormalization $g_{12}^*=g_{12}-f_{44}^2/c_{44}$ caused by the term $2f_{44}\frac{\partial u_{z\rho}}{\partial\rho}$ included into $f_3(u)$. Estimations for ferroelectric $PbTiO_3$ at room temperature gives $f_{44}^2/c_{44}\sim 10^{-11},\ldots,10^{-9}$ SI units, which is comparable with typical values of $g_{ij}\sim 10^{-10}$ SI units.[40] So, the renormalization cannot be neglected but the conditions $g_{ij}^*>0$ are necessary for the stability of the system without considering higher gradient terms [otherwise the single-domain state becomes unstable even at small $v_{ijklmn}(\partial u_{ij}/\partial x_k)(\partial u_{lm}/\partial x_n)$ values]. The perovskite ABO_3 lattice deformation caused by spontaneous flexoeffect in nanowires is shown in Fig. 1(a).

Typical values of external strain corresponding to the cantilever beam bending[12] are much smaller than the spontane-

ous one $u_{\rho z}=-(f_{44}/2c_{44})\partial\eta_3/\partial\rho$ caused by spontaneous flexoelectric effect near the surface $\rho=R$ of the nanowire [see Figs. 1(b) and 1(c)]. Besides the strain influences self-consistently on the order-parameter distribution, it should influence on all nanowire electromechanical and electronic properties related with its elastic state. The effect, originated from the inhomogeneity of the order parameter $\partial\eta_3/\partial\rho$, is the stronger, the smaller is the wire radius [compare curves 1–5 in Figs. 1(b) and 1(c)]. Similar effect should exist in thin ferroic nanotubes.

The analytical solution for elastic strain and displacements in thin pills (i.e., at $R \gg h$, $\partial\eta_3/\partial z \neq 0$, and $\partial\eta_3/\partial\rho \approx 0$) was derived in Appendix C in Ref. 39 as

$$u_{zz}(\rho,z)=\left[\frac{q_{11}}{c_{11}}\eta_3^2+\frac{2c_{12}}{c_{11}}\frac{(c_{12}q_{11}-c_{11}q_{12})\langle\eta_3^2\rangle}{(c_{11}^2+c_{11}c_{12}-2c_{12}^2)}+\frac{12(f_{12}c_{11}-c_{12}f_{11})}{(c_{11}^2+c_{12}c_{11}-2c_{12}^2)}\frac{2c_{12}}{c_{11}}\left\langle\frac{\partial\eta_3}{\partial z}\frac{z}{h}\right\rangle\frac{z}{h}-\frac{f_{11}}{c_{11}}\frac{\partial\eta_3}{\partial z}\right], \tag{8a}$$

$$u_z\left(\rho,z=\frac{h}{2}\right)=\frac{12(f_{12}c_{11}-c_{12}f_{11})}{(c_{11}^2+c_{12}c_{11}-2c_{12}^2)}\left\langle\frac{\partial\eta_3}{\partial z}\frac{z}{h}\right\rangle\frac{\rho^2}{2h}+h\left[\frac{q_{11}(c_{11}+c_{12})-2c_{12}q_{12}}{(c_{11}^2+c_{11}c_{12}-2c_{12}^2)}\right]\langle\eta_3^2\rangle. \tag{8b}$$

Here $\langle\varphi\rangle\equiv\frac{1}{h}\int_{-h/2}^{h/2}\varphi(z)dz$, where $\varphi(z)=\frac{\partial\eta_3}{\partial z}\frac{z}{h}$ or $\eta_3^2(z)$.

Substitution of elastic strain and displacement calculated from Eq. (8) into Eq. (5) leads to the renormalization of gradient coefficient g_{11} in Eq. (5) $g_{11}^*=g_{11}-f_{11}^2/c_{11}$ due to contribution of the last term $\frac{f_{11}}{c_{11}}\frac{\partial\eta_3}{\partial z}$ in Eq. (8a). The first term in Eq. (8b) corresponds to the parabolic particle bending induced by the flexoeffect [see Fig. 1(a)], while the second term is spontaneous strain independent on lateral coordinates (it could be also rewritten as $hQ_{11}\langle\eta_3^2\rangle$ and typically are much smaller than the first one starting from the radii $\rho > 1$ nm). So, the spontaneous flexoeffect leads to the transformation of the pill plain shape into the saucerlike one. The unique phenomenon can be considered as manifestation of spontaneous flexoeffect existence. We hope that it could be observed experimentally.

Allowing for the first term $f_{11}\frac{\partial^2 u_z}{\partial z^2}\equiv f_{11}\frac{\partial u_{zz}}{\partial z}$ in the function $f_3(u)$ introduced in Eq. (5) and expression for out-of-plane strain u_{zz} existing in thin pills, the appearance of *new terms* on the left-hand side of Eq. (5) was shown. Actually, in particular case of a thin pill ($R \gg h$) with symmetric conditions at boundaries $z=\pm h/2$, equation for the order-parameter distribution far from the boundary $\rho=R$ can be rewritten as (see Appendix C in Ref. 39)

$$\left(a_1-4q^2\langle\eta_3^2\rangle+qf\left\langle\frac{\partial\eta_3}{\partial z}\frac{z}{h}\right\rangle\frac{48}{h}z\right)\eta_3+f^2\left\langle\frac{\partial\eta_3}{\partial z}\frac{z}{h}\right\rangle\frac{24}{h}+b_{11}\eta_3^3-g_{11}^*\frac{\partial^2\eta_3}{\partial z^2}=E_0+E_3^d, \tag{9a}$$

where the following designations are introduced:

$$f=\frac{f_{12}c_{11}-c_{12}f_{11}}{\sqrt{c_{11}(c_{11}^2+c_{11}c_{12}-2c_{12}^2)}},$$

$$q=\frac{q_{12}c_{11}-q_{11}c_{12}}{\sqrt{c_{11}(c_{11}^2+c_{11}c_{12}-2c_{12}^2)}},$$

$$b_{11}=a_{11}-2\frac{q_{11}^2}{c_{11}}. \tag{9b}$$

Boundary conditions were obtained from Eq. (6) in the form

$$\left(\lambda^*\frac{\partial\eta_3}{\partial z}\pm\eta_3\right)\Bigg|_{z=\pm h/2}=0. \tag{9c}$$

Here we introduced the extrapolation length $\lambda^*=(g_{11}-\frac{f_{11}^2}{2c_{11}}-f^2)/a_1^S$ renormalized by flexoeffect.

Note that the new terms proportional to $\frac{f^2}{h}\langle\frac{\partial\eta_3}{\partial z}\frac{z}{h}\rangle$ and $qf\langle\frac{\partial\eta_3}{\partial z}\frac{z}{h}\rangle\frac{z}{h}\eta_3$, the latter is related to the flexostriction coupling contribution, were not considered previously[10–12] since it originates from the intrinsic inhomogeneity of order parameter in the nanostructures. Despite the nonlinear term $\langle\frac{\partial\eta_3}{\partial z}\frac{z}{h}\rangle\frac{z}{h}\eta_3$ does not lead to the transition temperature shift, our preliminary calculations showed that the term essentially influences (in comparison with conventional cubic term $\sim\eta_3^3$) the spatial distribution of η_3 in the ordered phase.

The distribution of relative vertical displacement u_z/h caused by flexoeffect for different values of pill thickness h and flexocoefficient f_{11} is shown in Figs. 2(b)–2(e) for an example of ferroelectric $PbTiO_3$. One can see that relative displacement decreases with pill thickness increase [compare curves 1–4 in parts (b) and (d)] and increases with flexoelectric coefficient increase [compare curves 1–4 in parts (c) and (e)]. The displacement profile is parabolic in agreement with Eq. (8b). Note that the first *flexoinduced* term in Eq. (8b) is negative, while the second striction term is positive for $PbTiO_3$ material parameters. For $\rho=0$ the displacement $u_z(0,z=\frac{h}{2})=h[\frac{q_{11}(c_{11}+c_{12})-2c_{12}q_{12}}{(c_{11}^2+c_{11}c_{12}-2c_{12}^2)}]\langle\eta_3^2\rangle$ depend on the thickness h but the numerical values of the different curves 1–4 vertical shift appeared $\sim 0.05-0.03$, so it is invisible in the linear scale. Note that boundary conditions (9c) are valid until $u_3 \ll h$. For small extrapolation lengths displacement increases more rapidly and becomes essential at higher thicknesses h [compare plots (a) and (b), and (c) and (d)]. In what follows we will consider the influence of flexoelectric effect on the properties of ferroelectric nanosystems in more detail, while the previous calculations are valid for other ferroics also.

IV. INFLUENCE OF SPONTANEOUS FLEXOELECTRIC EFFECT ON THE PROPERTIES OF NANOFERROELECTRICS

A. Thin pills

For specificity hereinafter we set $a_1(T)=\alpha_T(T-T_C)$ and use typical for screened ferroelectric thin pills depolarization field $E_3^d=(\langle P_3\rangle-P_3)/(\varepsilon_0\varepsilon_b)$, P_3 is polarization directed along the pill symmetry axes (see inset in Fig. 3), where ε_b is

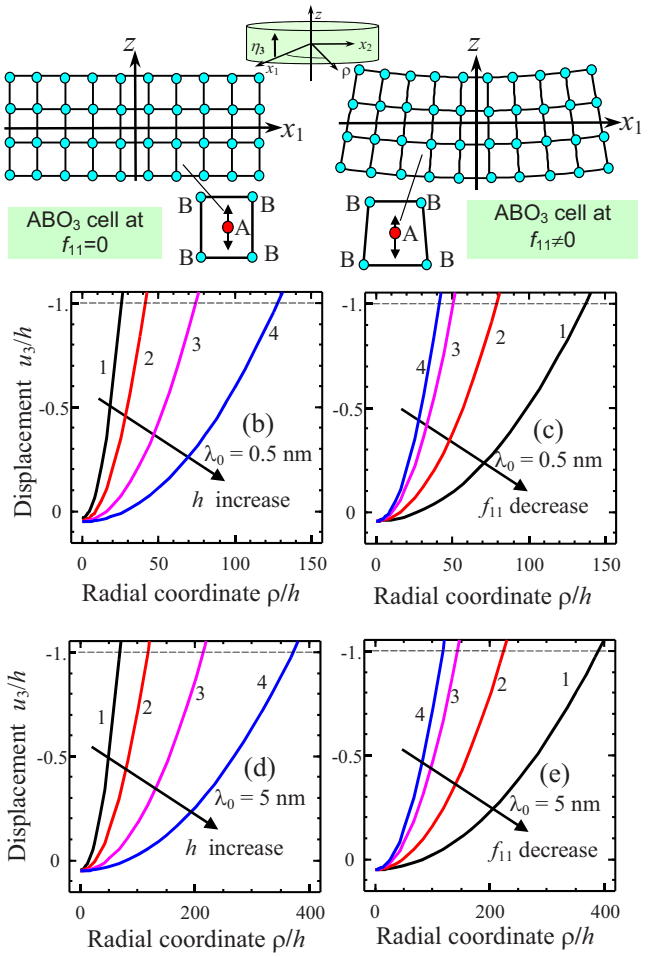

FIG. 2. (Color online) (a) Schematics of the perovskite ABO_3 lattice deformation caused by spontaneous flexoeffect in nanopills. [(b)–(e)] The distribution of vertical displacement for different values of pill thickness h=10, 30, 100, and 300 nm (curves 1–4); [(b) and (d)] flexoelectric coefficient for f_{11}=10 V; [(c) and (e)] h =30 nm, flexoelectric coefficient for f_{11}=1, 3, 7, and 10 V (curves 1–4); seeding extrapolation length [(b) and (c)] $\lambda_0 = g_{11}/a_1^S$ =0.5 nm and [(d) and (e)] 5 nm; and material parameters correspond to $PbTiO_3$.

dielectric permittivity of the background[41] or reference state[42] unrelated with ferroelectric soft mode (typically $\varepsilon_b < 10$). Linearized solution of Eq. (9a) gives the averaged value of susceptibility in paraelectric phase:

$$\langle \chi_{33} \rangle \approx \left[1 - \frac{2R_z^2}{(R_z + \lambda^*)h} \right] \left[a_1 + \frac{2g_{11}^*}{(R_z + \lambda^*)h} - \frac{24 f^2 R_z}{(R_z + \lambda^*)h^2} \right]^{-1}. \quad (10)$$

Here we introduced the characteristic length $R_z^2 = g_{11}^* \varepsilon_0 \varepsilon_b$ (see Appendix C in Ref. 39 for details). Equation (10) was derived for typical condition $h \gg R_z$. Using the divergence of susceptibility [Eq. (10)], one could find the critical temperature of the transition between paraelectric and ferroelectric phases:

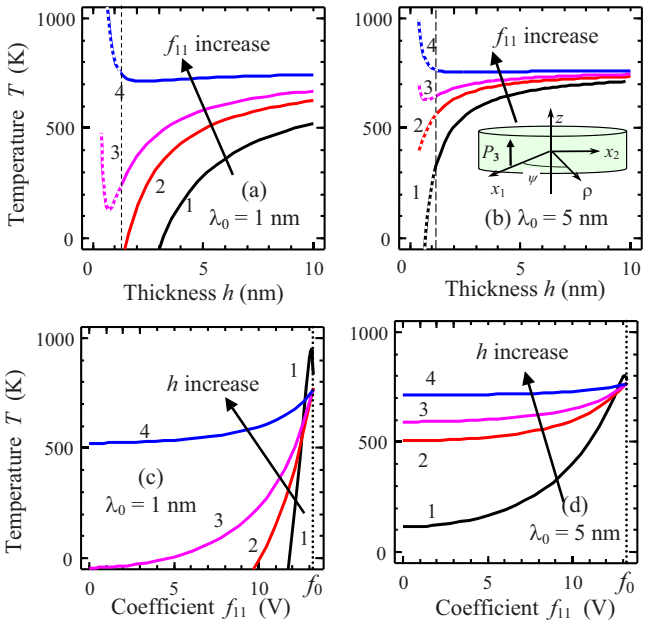

FIG. 3. (Color online) [(a) and (b)] The dependence of transition temperature T_{cr} on pill thickness h for different values of flexoelectric coefficient f_{11}=0, 11, 12, and 13 V (curves 1–4). [(c) and (d)] The dependence of transition temperature T_{cr} on flexoelectric coefficient for different values of thickness h=0.8, 2, 3, and 10 nm (curves 1–4). Seeding extrapolation length [(a) and (c)] $\lambda_0 = g_{11}/a_1^S$=1 nm and [(b) and (d)] 5 nm, material parameters correspond to $PbTiO_3$: $g_{11}=10^{-9}$ J m^3/C^2, ε_b=1, T_C=765 K, $\alpha_T = 7.53\times10^6$ J m/C^2 K, $c_{11}=1.75\times10^{11}$ J/m^3, and $c_{12}=0.79\times10^{11}$ J/m^3.

$$T_{cr}(h, f_{11}) \approx T_C - \frac{1}{\alpha_T}\left[\frac{2g_{11}^*}{(R_z + \lambda^*)h} - \frac{24 f^2 R_z}{(R_z + \lambda^*)h^2} \right]. \quad (11)$$

The first term in Eq. (11) is the bulk transition temperature, the second term is mainly determined by the influence of surface effects and depolarization field renormalized by the flexoeffect. The third term originated from the influence of the flexoterm $\sim \frac{f^2}{h}\langle \frac{\partial P_3}{\partial z} \frac{z}{h} \rangle$ in Eq. (9a). It should be noted that the signs of these terms are different, so, while the second term leads to the critical temperature suppression, the third one always increases the temperature.

The transition temperature nonmonotonic behavior, namely, minimum at thickness $h_{min} = 24 f^2 R_z / g_{11}^*$, followed by increase at the smallest thickness values appeared for high values of flexoelectric coefficient f_{11} are related to the third term in Eq. (11) that is inversely proportional to h^2. Despite the term is negligible at higher thicknesses, its contribution to the transition temperature dominates over the second term proportional to $1/h$ at small thickness values. However, one should restrict consideration for the thickness greater than several lattice constants; otherwise phenomenological approach can be inapplicable (see Sec. I). Since h_{min} value depends on the material parameters and so it is not excluded that for some materials h_{min} can be in the region of phenomenological theory applicability. The ferroelectric transition temperature dependence on thickness h and flexoelectric co-

efficient f_{11} calculated from exact expression (C.21) from Appendix C in Ref. 39 is shown in Fig. 3.

However, for the small flexoelectric coefficients values $h_{\min}$ is usually smaller than several lattice constants, so the effect of T_{cr} nonmonotonic behavior predicted within Landau-Ginzburg-Devonshire phenomenological approach may be unrealistic [see dotted parts of curves 1–4 in the region of ultrasmall thickness in Figs. 3(a) and 3(b)]. However, for the higher values of flexoelectric coefficient f_{11}, and so $h_{\min}$ values, the transition temperature $T_{cr}(h,f_{11})$ is rather high at $h=h_{\min}$, so the disappearance of thickness-induced phase transition induced by flexoelectric coupling in ferroelectric pills can be reliably predicted within the phenomenology [see curves 3 and 4 in Figs. 3(a) and 3(b)]. The influence of the extrapolation length on the transition temperature and flexoelectric coupling effect is obvious: for small extrapolation lengths, size effects are more pronounced and become essential at higher thicknesses h [compare plots (a) and (b)].

The effect of transition temperature increase with flexoelectric coefficient f_{11} increase is demonstrated in Figs. 3(c) and 3(d) for several fixed thicknesses h. The smaller is the thickness h, the higher is the slope of $T_{cr}(f_{11})$ dependence [compare curves 1–4 in Figs. 3(c) and 3(d)]. Temperature $T_{cr}(f_{11})$ increases with thickness h increase until $h \gg h_{\min}$ [compare curves 4, 3, and 2 in Figs. 3(c) and 3(d)]. For ultrathin pills with thickness $h \leq h_{\min}$ nonmonotonic effects appeared [see maximum at curve 1 in Figs. 3(c) and 3(d)]. For smaller extrapolation lengths, size effects are more pronounced and become essential at higher thicknesses h [compare plots (c) and (d)]. Note that all curves in Figs. 3(c) and 3(d) have physical meaning until flexoelectric coefficient f_{11} is smaller than the limiting value $f_0=\sqrt{g_{11}c_{11}}$.

Actually, analytical expression [Eq. (11)] provides quantitative information about the spontaneous flexoeffect contribution into the transition temperature in ferroic nanopills. What is the simple physical meaning of flexoeffect induced increase in the phase-transition temperature? The reasonable explanation is the "ordering" role of the new term $\frac{f^2}{h}\langle\frac{\partial P_3}{\partial z}\frac{z}{h}\rangle$ *linear* on the order parameter P_3. The flexoinduced deformation of the ABO_3 unit-cell vertical cross section [shown in Fig. 2(a)] stimulates the polar-active displacement of central B cation and thus increases paraelectric phase instability. However, linearized solution of Eq. (9a) was obtained in the assumption that the pill surfaces $z=\pm h/2$ remained almost flat [see the boundary conditions (9c)]. Rigorously, it is approximation valid until $u_3 \ll h$ since flexoeffect leads to the pill edges bending [as shown in Figs. 2(b)–2(d)]. In Sec. V we demonstrate that although the terms like $\langle\frac{\partial P_3}{\partial z}\frac{z}{h}\rangle$ and $\langle\frac{\partial P_3}{\partial z}\frac{z}{h}\rangle\frac{z}{h}\eta_3$ are absent for ferroelectric nanowire with order parameter directed along its axis flexoelectric effect essentially influences nanowire properties.

B. Nanowires

Below we demonstrate that the renormalization of gradient coefficient and extrapolation length strongly affects all the properties and in particular the transition temperature shift and correlation radius in single-domain ferroelectric nanowires with axial symmetry of the polarization P_3 [see Fig. 4(a)]. For short-circuit boundary conditions $E_3^d(\rho,z) \approx [1+(h/2R)^2]^{-1}[\bar{P}_3-P_3(\rho,z)]/(\varepsilon_0\varepsilon_b)$,[43] while $E_3^d(\rho,z) \approx -[1+(h/2R)^2]^{-1}P_3(\rho,z)/(\varepsilon_0\varepsilon_b)$ for the open-circuit ones. So, one can neglect small depolarization field $E_d \sim (R/h)^2$ for the case $h \gg R$ typical for nanowires.

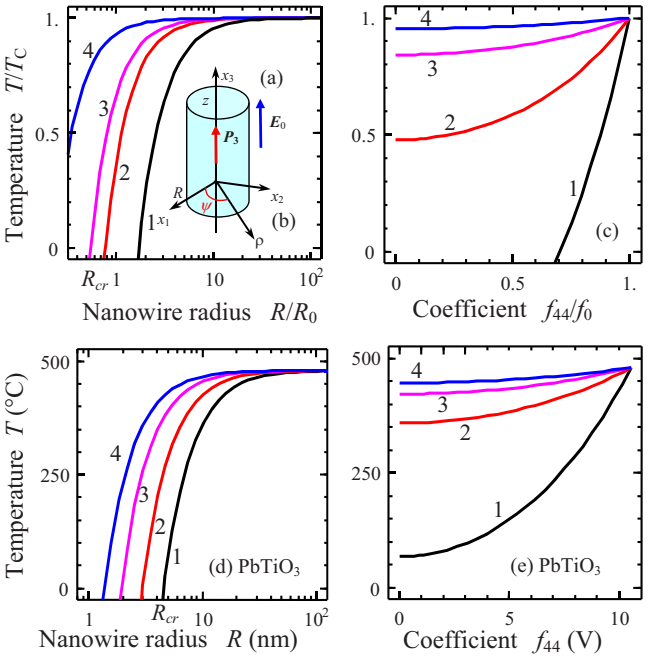

FIG. 4. (Color online) (a) Nanowire with cylindrical coordinates defined as (ρ,ψ,z). [(b) and (c)] Phase-transition temperature T_{cr} dependence vs the nanowire radius at fixed flexoelectric coefficient $f_{44}/f_0=0$, 0.9, 0.95, and 0.99 (curves 1–4) and (c) T_{cr} dependence on flexoelectric coefficient at fixed radius $R/R_c=1.25$, 2.5, 5, and 10 (curves 1–4). Parameter $g_{12}/(a_1^S R_c)=1$. [(d) and (e)] Transition temperature T_{cr} dependence on radius (d) at fixed values of flexoelectric coefficient $f_{44}=0$, 8, 9.5, and 10 V (curves 1–4) and dependence on flexoelectric coefficient (e) at fixed values of radius $R=5$, 10, 15, and 20 nm (curves 1–4). $PbTiO_3$ material parameters $T_c=479$ °C, $\alpha_T=3.8\times10^5$ J m/C^2 K, $c_{44}=1.1\times10^{11}$ J/m^3, $g_{12}=10^{-9}$ J m^3/C^2, and seeding extrapolation length $\lambda_0=1$ nm.

Substitution of Eq. (7) into Eq. (5) leads to the Euler-Lagrange equation for the polarization $P_3(\rho)$:

$$a_1(T)P_3 - g_{12}^*\left(\frac{d^2P_3}{d\rho^2}+\frac{1}{\rho}\frac{dP_3}{d\rho}\right)+\left(a_{11}-\frac{q_{12}^2}{c_{11}}\right)P_3^3+b_{11}\overline{P_3^2}P_3 = E_0. \tag{12}$$

Renormalized coefficient

$$b_{11}=-\frac{q_{11}^2(c_{11}+c_{12})c_{11}+(c_{11}^2-c_{11}c_{12}+2c_{12}^2)q_{12}^2-4c_{11}c_{12}q_{11}q_{12}}{c_{11}(c_{11}-c_{12})(c_{11}+2c_{12})}.$$

The boundary conditions (6) can be rewritten via renormalized extrapolation length λ^* as

$$\left[P_3+\lambda^*(R)\frac{dP_3}{d\rho}\right]\Bigg|_{\rho=R}=0, \tag{13a}$$

$$\lambda^*(R) = \frac{g_{12}}{a_1^S(R)}\left(1 - \frac{f_{44}^2}{2c_{44}g_{12}}\right) = \frac{4R\lambda_0}{4R - 2a + 5\lambda_0}\left(1 - \frac{f_{44}^2}{2c_{44}g_{12}}\right). \tag{13b}$$

In Eq. (13b) we used that the "seeding" extrapolation length $\lambda(R)=g_{12}/a_1^S(R)$ depends on the rod radius R and material lattice constant a as $\lambda(R)=\frac{4R\lambda_0}{4R-2a+5\lambda_0}$ in accordance with Wang and Smith calculations.[18] Here λ_0 has the meaning of extrapolation length of semi-infinite ferroelectric material.

So, for nanowires flexoelectric effect leads to the renormalization of the gradient coefficient and extrapolation length. This means that in order to consider the spontaneous flexoelectric effect influence on the properties one has to rewrite all the analytical expressions obtained earlier for long nanorods and nanowires physical properties without flexoelectric effect[14,44] by the substitution g_{12}^* and λ^* for g and λ_S in the expressions for the corresponding property. In what follows we will demonstrate the spontaneous flexoeffect influence on the critical parameters (temperature and radius) of size-induced phase transition and correlation radius using the results[14,44] obtained without flexoeffect.

Approximate expression for ferroelectric to the paraelectric phase-transition temperature $T_{cr}(R)$ for nanowires could be rewritten as

$$T_{cr}(R,f_{44}) \approx \begin{cases} T_C - \dfrac{2}{\alpha_T}\left[\dfrac{g_{12}^*}{R\lambda^*(R) + 2R^2/k_{01}^2}\right], & \lambda^* > 0 \\ T_C - \dfrac{2}{\alpha_T}\left[g_{12}^*\dfrac{2\lambda^*(R) - R}{2R\lambda^{*2}}\right], & \lambda^* < 0, \end{cases} \tag{14}$$

where $k_{01}=2.408\cdots$ is the smallest positive root of equation $J_0(k)=0$. Renormalized transition temperature T_{cr} dependences vs nanowire radius and flexoelectric coefficients f_{44} are shown in Figs. 4(b) and 4(c) for dimensionless variables and in Figs. 4(d) and 4(e) for $PbTiO_3$ material parameters. It is clear from the plots that the higher is the f_{44} value, the higher is the transition temperature T_{cr} and the smaller is the critical radius R_{cr} that corresponds to $T=T_{cr}$.

An approximate analytical expression for the critical radius was derived from Eq. (14) under the assumption $R \geq \lambda_0$:

$$R_{cr}(T,f_{44}) \approx \sqrt{\left(1 - \frac{f_{44}^2}{f_0^2}\right)k_{01}^2R_0^2\frac{T_C}{T_C - T} + \left(\frac{f_{44}^2}{2f_0^2} - 1\right)^2 k_{01}^4\frac{\lambda^{*2}}{16}} - k_{01}^2\frac{\lambda^*}{4}\left(1 - \frac{f_{44}^2}{2f_0^2}\right). \tag{15}$$

Here $f_0=\sqrt{g_{12}c_{44}}$, $\lambda^*(R)\approx\lambda_0(1-f_{44}^2/2c_{44}g_{12})$, and $R_b=\sqrt{g_{12}/\alpha_T T_c}$ is the bulk correlation radius at zero temperature. Under the condition $R<\lambda_0$ the critical radius should be calculated numerically from Eq. (14) as the solution of equation $T_{cr}(R_{cr},f_{44})=0$. Critical radius R_{cr} dependence on flexoelectric coefficients f_{44} for different temperatures is shown in Fig. 5. Solid curves calculated numerically from Eq. (14) are very closed to dashed curves calculated from Eq. (15). So, it is clear that approximation [Eq. (15)] works surprisingly well. Thus, flexoelectric effect renormalizes both critical temperature and critical radius.

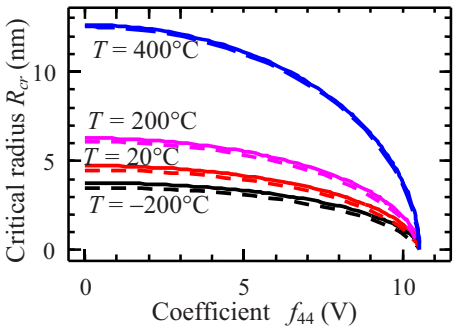

FIG. 5. (Color online) Critical radius R_{cr} vs flexoelectric coefficients f_{44} for different temperatures $T=-20$, 20, 200, and 400 °C (marked near the curves). Solid curves are calculated numerically from Eq. (14); dashed curves are calculated from analytical Eq. (15). $PbTiO_3$ material parameters are the same as in Fig. 4.

Let us underline that at radii slightly higher than the critical one the region of the almost vertical slope of the dependences $T_{cr}(R)$ drastically increases with f_{44} increase [compare curves 1 and 4 in Fig. 4(b)]. For chosen material parameters the increase in the slope caused by the flexoelectric coefficient increase on several percents leads to the increase in transition temperature in 2–3 times. With the rod radius increase the terms related with the flexoelectric effect decreases as $1/R$ and becomes unessential at radii $R \gg R_{cr}$ [curves 1–4 in Figs. 4(b) and 4(d) calculated at different f_{44} converge together and tend to the bulk value with radius increase].

Application of the direct variational method[14,43] for the Euler-Lagrange equation (12) leads to the conventional form of the free energy with renormalized coefficients

$$F_R(\bar{P}_3) \approx \alpha_T[T - T_{cr}(R)]\frac{\bar{P}_3^2}{2} + \left(a_{11} - \frac{q_{12}^2}{c_{11}} + b_{11}\right)\frac{\bar{P}_3^4}{4} - \bar{P}_3E_0. \tag{16}$$

It is seen that because the critical temperature $T_{cr}(R)$ in Eq. (14) depends on the flexoelectric coupling coefficient f_{44}, the average polarization $\bar{P}_3$ and all other physical properties determined by it have to be dependent on the flexoelectric coefficient f_{44}. Note that $\bar{P}_3$ and other physical properties can be found by the conventional minimization of the free energy [Eq. (16)].

The main effect from the flexoelectric coupling is the change in transition temperature via the renormalization of the extrapolation length and the gradient term [see Eq. (14)]. Because of the same reasons flexoelectric coupling will lead to the renormalization of correlation radius as

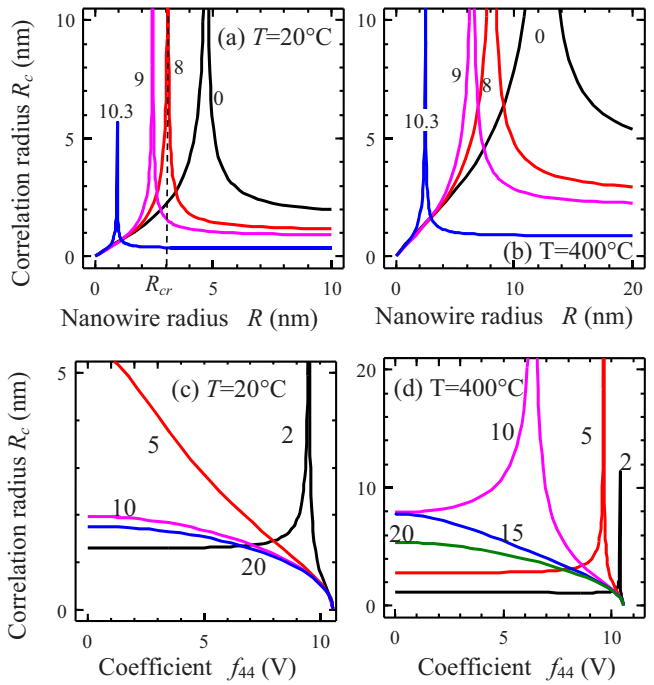

FIG. 6. (Color online) [(a) and (b)] Correlation radius dependences vs nanowire radius for different flexoelectric coefficients f_{44} marked near curves (in V) and T=20 and 400 °C. [(c) and (d)] Correlation radius dependences vs flexoelectric coefficients f_{44} for different wire radius marked near curves (in nm) and T=20 and 400 °C. $PbTiO_3$ material parameters are the same as in Fig. 4.

$$R_c^*(T,R,f_{44}) = \begin{cases} \sqrt{\dfrac{g_{12}-f_{44}^2/c_{44}}{\alpha_T[T-T_{\rm cr}(R,f_{44})]}} & \text{paraelectric phase} \\ \sqrt{-\dfrac{g_{12}-f_{44}^2/c_{44}}{2\alpha_T[T-T_{\rm cr}(R,f_{44})]}} & \text{ferroelectric phase.} \end{cases} \quad (17)$$

The renormalized correlation radius dependences vs nanowire radius and flexoelectric coefficients f_{44} are shown in Figs. 6(a)–6(d) for $PbTiO_3$ material parameters at room temperature.

The divergences of correlation radius could be achieved only for $T=T_{\rm cr}(R,f_{44})$ or at $R=R_{\rm cr}$, corresponding to the paraelectric-ferroelectric phase-transition point as one can see from Eq. (17). These conditions can be fulfilled at fixed value of radius R for arbitrary value f_{44} or for arbitrary value of radius at given value of temperature T, as one can see from Fig. 6. Since the same fixed values of R or f_{44} correspond to the divergence (or maxima for finite electric field value) of dielectric permittivity χ (because $R_c^* \sim \sqrt{g_{12}^*\chi}$) these values of the radius and flexoelectric coefficient represent the critical radius or "critical" flexoelectric coefficient [corresponding to $R_{\rm cr}$ given by Eq. (15)] of the paraelectric-ferroelectric phase transition.

It is clear from Figs. 6(a) and 6(b) that in ferroelectric phase (i.e., at $R>R_{\rm cr}$) the correlation radius monotonically decreases with the increase in the flexoelectric coefficient f_{44}. At the same time, in paraelectric phase correlation radius increases with the increase in the flexoelectric coefficient since the critical temperature [Eq. (14)] increases with the increase in the flexoelectric coefficient. This opens the possibility to govern the phase diagram and polar properties by the choice of the material with necessary flexoelectric coefficient at given temperature or nanoparticle radius.[45]

Finally, let us calculate the nanowire *piezoelectric reaction* to electric field E_3 applied along the polar axes z. Using the elastic field [Eq. (7)], one could calculate piezoelectric reaction as $d_{kij}=\partial u_{ij}/\partial E_k$. One of the nontrivial consequences of the flexoeffect is the *local appearance* of *new* piezoelectric tensor components, related with the *unit-cell deformation* [see Fig. 1(a)], absent in the bulk system

$$d_{331}=d_{313}=-\frac{f_{44}}{2c_{44}}\frac{\partial\chi_{33}}{\partial\rho}\cos\varphi,$$

$$d_{332}=d_{323}=-\frac{f_{44}}{2c_{44}}\frac{\partial\chi_{33}}{\partial\rho}\sin\varphi. \quad (18)$$

Here χ_{33} is dielectric susceptibility and φ is the polar angle. The flexoinduced part of the piezoelectric reaction amplitude is proportional to

$$d_{33\rho}(T,R) \sim \frac{f_{44}}{2\alpha_T[T_{\rm cr}(R)-T]}\left[\frac{J_1(\rho/R_0)}{R_0J_0(R/R_0)-(\lambda^*/R_0)J_1(R/R_0)}\right], \quad (19)$$

where radius $R_0=\sqrt{g_{12}^*/\alpha_T(T-T_C)}$. As anticipated $d_{33\rho}(T,R)$ diverges in the point $T=T_{\rm cr}(R)$ of size-induced paraelectric-ferroelectric phase transition. It is clear from Figs. 7(c) and 7(d) the piezoresponse is the higher the smaller is the wire radius (compare curves 1–6).

Note that the flexocontribution [Eq. (19)] is proportional to $[T_{\rm cr}(R)-T]^{-1}$, so it can be much greater than the striction contribution $d_{3ij}\sim -2q_{ij33}P_3\chi_{33}$ proportional to the $[T_{\rm cr}(R)-T]^{-1/2}$ near the size-induced phase-transition point $T=T_{\rm cr}(R)$. Thus, spontaneous flexoeffect originated from the intrinsic gradient $\partial P_3/\partial\rho$ of the order parameter near the wire surface could lead to *giant piezoelectric reaction.* It should be noted that measured coefficient of proportionality between strain gradient and polarization is $\chi_{33}f_{ij3l}$.[8]

V. DISCUSSION

The intrinsic inhomogeneity of order parameter in the ferroic nanosystems due to the surface and size effects is the source of the spontaneous flexocoupling with mechanical strain (e.g., flexoelectric and flexomagnetic effects). Thus it has to be taken into account when calculating polar properties of the nanosystems and their response to the external stimuli.

The exact analytical solution for the spatially inhomogeneous mechanical displacement vector allowing for flexoeffect contribution was derived for nanowires and pills with one-component vector order parameter η_3 directed along the nanoparticle symmetry axis. We show that flexoeffect leads

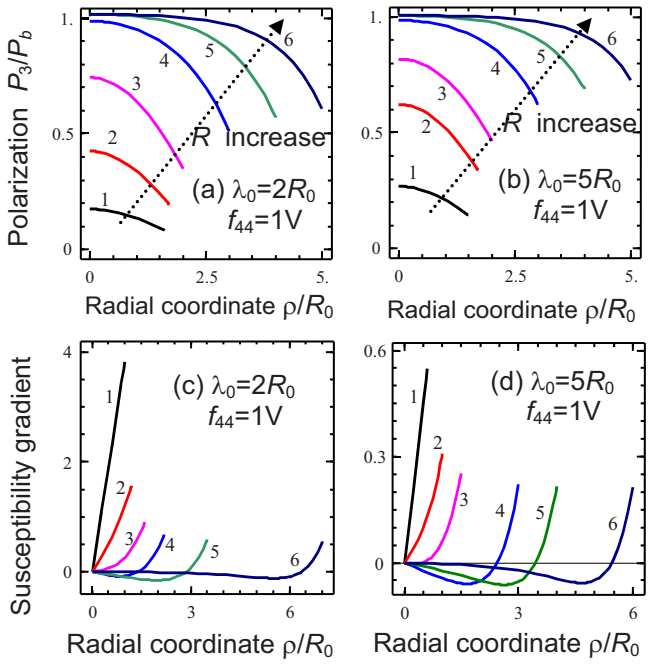

FIG. 7. (Color online) [(a) and (b)] Polarization distribution inside the nanorods with flexoelectric coefficient $f_{44}=1$ V. Lattice constant $a<0.5R_0$, different values of seeding extrapolation length (a) $\lambda_0=2R_0$ and (b) 5 and nanorod radius values $R/R_0=1.615$, 1.7, 2, 3, 4, and 5 [curves 1–6 in plot (a)] and $R/R_0=1.5$, 1.7, 2, 3, 4, and 5 [curves 1–6 in plot (b)]. Here $P_b=\sqrt{-\alpha_T(T-T_c)/a_{11}}$ is spontaneous polarization of the bulk material. [(c) and (d)] Normalized susceptibility gradient $(\partial\chi_{33}/\partial\rho)\chi_b^{-1}R_0$ inside the nanorod of different radii R for flexoelectric coefficient $f_{44}=1$ V and $PbTiO_3$ material parameters. Lattice constant $a<0.5R_0$, different values of seeding extrapolation length (a) $\lambda_0=2R_0$ and (b) 5, and nanorod radius values $R/R_0=1$, 1.2, 1.6, 2.2, 3.5, 7, and 10 curves 1–6 in plot (a)] and $R/R_0=0.6$, 1, 1.5, 3, 4, and 6 [curves 1–6 in plot (b)].

to the appearance of two additional terms in the equation of state for the order parameter η_3, proportional to its first derivative, and the third term proportional to its second derivative. These terms, respectively, cause the appearance of linear term $\sim\langle x_3\partial\eta_3/\partial x_3\rangle$ and nonlinear contribution $\sim\eta_3\langle x_3\partial\eta_3/\partial x_3\rangle$ in thin pills, the renormalization of coefficients before the order-parameter gradient $\partial^2\eta_3/\partial x_i\partial x_j$ as well as result in inhomogeneity and renormalization of extrapolation length in the boundary conditions for pills and nanowires. Estimations show that these effects cannot be neglected.

The spontaneous flexoeffect leads to the transformation of the unit-cell symmetry (e.g., from the squire cross section to trapezoid one) of rods and pills that changes their plane cross sections into the saucerlike one. This phenomenon can be considered as manifestation of spontaneous flexoeffect existence. The forecast is waiting for experimental verification.

The influence of flexoeffect on the nanosystem properties was considered in detail for the most studied flexoelectric effect. One can conclude that even a rather moderate flexoelectric effect significantly renormalizes all the polar, piezoelectric, and dielectric properties and in particular the correlation radius suppresses the size-induced phase transition from ferroelectric to paraelectric phase and thus stabilizes the ordered phase in ferroic nanoparticles.

The divergences of dielectric permittivity and correlation radius at the critical value of the flexoelectric coefficient related to the critical radius had shown a way to govern ferroelectric materials properties. The effect of the correlation radius renormalization by the flexoelectric effect leads to the changes in the domain-wall intrinsic width. The predicted effects are useful for design of ferroelectric nanowires with radius up to several nanometers, which have ultrathin domain walls and reveal close to bulk polar properties.

*Corresponding author.
†eliseev@i.com.ua
‡Permanent address: V. Lashkarev Institute of Semiconductor Physics, NAS of Ukraine, 41, pr. Nauki, 03028 Kiev, Ukraine; morozo@i.com.ua

[1] Sh. M. Kogan, Sov. Phys. Solid State **5**, 2069 (1964).
[2] A. K. Tagantsev, Phys. Rev. B **34**, 5883 (1986).
[3] A. K. Tagantsev, Phase Transitions **35**, 119 (1991).
[4] R. Sabirianov and P. Lukashev, Materials Research Society Fall Meeting, Boston MA, 1–4 December 2008 (unpublished), Paper No. K5.7.
[5] V. S. Mashkevich and K. B. Tolpygo, Zh. Eksp. Teor. Fiz. **31**, 520 (1957) [Sov. Phys. JETP **4**, 455 (1957)].
[6] W. Ma and L. E. Cross, Appl. Phys. Lett. **79**, 4420 (2001).
[7] W. Ma and L. E. Cross, Appl. Phys. Lett. **81**, 3440 (2002).
[8] W. Ma and L. E. Cross, Appl. Phys. Lett. **82**, 3293 (2003).
[9] P. Zubko, G. Catalan, P. R. L. Welche, A. Buckley, and J. F. Scott, Phys. Rev. Lett. **99**, 167601 (2007).
[10] G. Catalan, L. J. Sinnamon, and J. M. Gregg, J. Phys.: Condens. Matter **16**, 2253 (2004).
[11] G. Catalan, B. Noheda, J. McAneney, L. J. Sinnamon, and J. M. Gregg, Phys. Rev. B **72**, 020102(R) (2005).
[12] M. S. Majdoub, P. Sharma, and T. Cagin, Phys. Rev. B **77**, 125424 (2008).
[13] S. V. Kalinin and V. Meunier, Phys. Rev. B **77**, 033403 (2008).
[14] M. D. Glinchuk, E. A. Eliseev, A. N. Morozovska, and R. Blinc, Phys. Rev. B **77**, 024106 (2008).
[15] D. R. Tilley, in *Ferroelectric Thin Films*, edited by C. Paz de Araujo, J. F. Scott, and G. W. Teylor (Gordon and Breach, Amsterdam, 1996).
[16] A. S. Sidorkin, *Domain Structure in Ferroelectrics and Related Materials* (Cambridge International Science, Cambridge, 2006).
[17] G. Geneste, E. Bousquest, J. Junquera, and P. Chosez, Appl. Phys. Lett. **88**, 112906 (2006).
[18] C. L. Wang and S. R. P. Smith, J. Phys.: Condens. Matter **7**, 7163 (1995).
[19] A. Sundaresan, R. Bhargavi, N. Rangarajan, U. Siddesh, and C. N. R. Rao, Phys. Rev. B **74**, 161306(R) (2006).
[20] E. Erdem, H.-Ch. Semmelhack, R. Bottcher, H. Rumpf, J. Banys, A. Matthes, H.-J. Glasel, D. Hirsch, and E. Hartmann, J.

Phys.: Condens. Matter **18**, 3861 (2006).
[21] D. Yadlovker and S. Berger, Phys. Rev. B **71**, 184112 (2005).
[22] D. D. Fong, G. B. Stephenson, S. K. Streiffer, J. A. Eastman, O. Auciello, P. H. Fuoss, and C. Thompson, Science **304**, 1650 (2004).
[23] M. S. Majdoub, R. Maranganti, and P. Sharma, Phys. Rev. B **79**, 115412 (2009).
[24] M. E. Lines and A. M. Glass, *Principles and Applications of Ferroelectrics and Related Phenomena* (Clarendon, Oxford, 1977).
[25] M. I. Kaganov and A. N. Omelyanchouk, Zh. Eksp. Teor. Fiz. **61**, 1679 (1971) [Sov. Phys. JETP **34**, 895 (1972)].
[26] I. Rychetsky, J. Phys.: Condens. Matter **9**, 4583 (1997).
[27] S. P. Alpay, I. B. Misirlioglu, A. Sharma, and Z.-G. Ban, J. Appl. Phys. **95**, 8118 (2004).
[28] Z. G. Ban, S. P. Alpay, and J. V. Mantese, Phys. Rev. B **67**, 184104 (2003).
[29] G. Akcay, S. P. Alpay, G. A. Rossetti, and J. F. Scott, J. Appl. Phys. **103**, 024104 (2008).
[30] Q. Y. Qiu, V. Nagarajan, and S. P. Alpay, Phys. Rev. B **78**, 064117 (2008).
[31] V. I. Marchenko and A. Ya. Parshin, Zh. Eksp. Teor. Fiz. **79**, 257 (1980) [Sov. Phys. JETP **52**, 129 (1980)].
[32] V. A. Shchukin and D. Bimberg, Rev. Mod. Phys. **71**, 1125 (1999).
[33] M. D. Glinchuk, A. N. Morozovska, and E. A. Eliseev, J. Appl. Phys. **99**, 114102 (2006).
[34] L. D. Landau and E. M. Lifshitz, *Theory of Elasticity. Theoretical Physics* (Butterworth-Heinemann, Oxford, UK, 1998), Vol. 7.
[35] G. A. Smolenskii, V. A. Bokov, V. A. Isupov, N. N. Krainik, R. E. Pasynkov, and A. I. Sokolov, *Ferroelectrics and Related Materials* (Gordon and Breach, New York, 1984).
[36] L. D. Landau and E. M. Lifshits, *Electrodynamics of Continuous Media* (Butterworth- Heinemann, Oxford, 1980).
[37] R. Kretschmer and K. Binder, Phys. Rev. B **20**, 1065 (1979).
[38] S. P. Timoshenko and J. N. Goodier, *Theory of Elasticity* (McGraw-Hill, New York, 1970).
[39] E. A. Eliseev, A. N. Morozvska, M. D. Glinchuk, and R. Blinc, arXiv:0811.1031 (unpublished).
[40] Measurable value is $\eta(T)=f_{44}/a_1(T)$ relating the strain gradient with polarization. It was estimated in the papers of Ma and Cross (Refs. 6–8) and Zubko *et al.* (Ref. 9) as $\eta(T) \sim 10^{-9},\ldots,10^{-6}$ C/m. For PTO $a_1(T) \approx -2\times 10^{-8}$ SI units at room temperature.
[41] A. K. Tagantsev and G. Gerra, J. Appl. Phys. **100**, 051607 (2006).
[42] C. H. Woo and Y. Zheng, Appl. Phys. A **91**, 59 (2007).
[43] A. N. Morozovska, E. A. Eliseev, and M. D. Glinchuk, Phys. Rev. B **73**, 214106 (2006).
[44] A. N. Morozovska, M. D. Glinchuk, and E. A. Eliseev, Phys. Rev. B **76**, 014102 (2007).
[45] Note that for polydomain (if any) wires the predicted effect of R_c^* decrease with f_{44} increase should lead to the decrease in the intrinsic domain-wall width defined as $2R_c^*$.